***Proceedings of the IASS 2024 Symposium***
*Redefining the Art of Structural Design*
August 26-30, 2024, Zurich Switzerland
Philippe Block, Giulia Boller, Catherine DeWolf,
Jacqueline Pauli, Walter Kaufmann (eds.)

# Origami-based flat foldable structure with non-flat singular point of rigid folding mechanism

Kentaro HAYAKAWA*, Makoto OHSAKI

* Department of Architecture and Architectural Engineering, Kyoto University
Kyoto-Daigaku Katsura, Nishikyo, Kyoto 615-8540, Japan
se.hayakawa@archi.kyoto-u.ac.jp

## Abstract

We introduce an origami-based rigid- and flat-foldable structure that has an isolated singular state of mechanism in the non-flat state. The structure consists of a grid of units arranged on a plane, each of which is a ring of eight right-angled isosceles triangles with eight crease lines corresponding to one layer of the Yoshimura Tube. Adjacent units, which are inverted upside down, are connected by gluing a face of one unit to a face of the other so that the vertex of 90 degrees of one face coincides with the center point of the longest edge of the other face. The thickness of each face can be easily assigned by offsetting the face to the outside direction of the unit and by arranging hinges at the inside of the unit. In this study, we investigate properties of the proposed structure using the panel-pin model developed for the analysis of rigid origami. In the case of a structure with three or more units in both directions of the grid, it has one in-plane finite mechanism and one out-of-plane first-order infinitesimal mechanism in the singular state where all folding angles are equal. However, in other non-flat states, it has only one in-plane finite mechanism. By utilizing this property, the structure can be compactly stored in a flat state and stably deployed while the out-of-plane mechanism in the singular state may realize a curved surface structure.

**Keywords**: rigid origami, flat foldable, thick panel, singular state

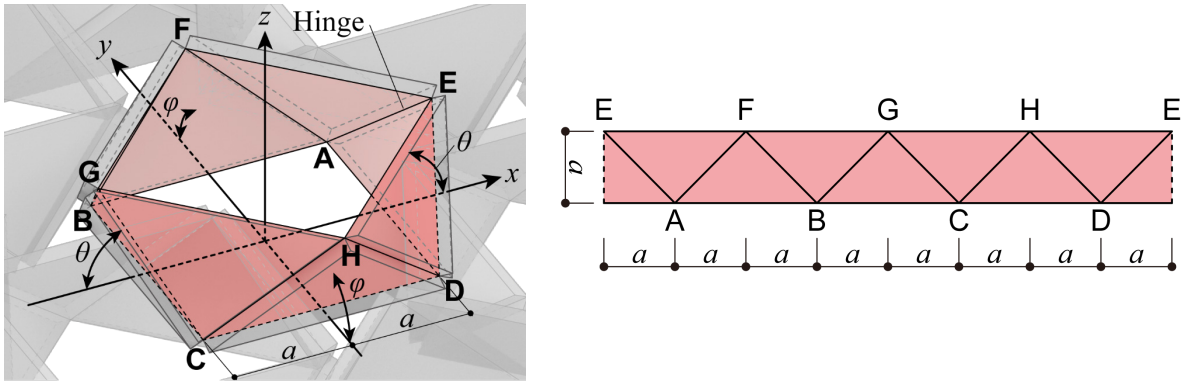


(a) (b)

Figure 1. Geometry of a single unit: (a) dimension of the unit, labelling of vertices, and variables representing the folding states on the primary path in the isometric view, (b) development diagram of the unit cut at vertex E.

## 1. Introduction

Origami in the strict definition refers to the technique of creating two- or three-dimensional shapes by simply folding a single thin sheet such as a piece of paper without cutting or pasting it. However, a broader definition is often employed in the engineering field; we also refer to structures obtained by

allowing cutting and pasting as origami structures when the technique of folding is used. For example, origami tubes [1–3] are tubular structures with crease lines, which are often used as energy absorption devices and stiff, yet reconfigurable structures. Sandwich panels with cores manufactured by using an origami technique, called origami honeycombs or origami cores [4–6], are lightweight, stiff, and highly manufacturable. Origami technique similar to the origami honeycomb is also utilized for the design and construction of the sculptures and the architectural surfaces [7].

In this paper, we introduce an origami-based rigid- and flat-foldable structure that is not manufactured from a single sheet of paper. Figure 1 illustrates a unit of the proposed structure. The entire structure is formed by arranging it as shown in Fig. 2 in a grid manner on a plane. A single unit is a ring of eight right-angled isosceles triangles with eight crease lines corresponding to the special case of 8R linkage or one layer of the Yoshimura Tube [3]. When the axial direction of the unit corresponds to the $z$-axis in Fig. 1, adjacent units are connected in the following manners:

- The axes of the adjacent units are parallel, but these units are inverted upside down.
- Between the glued faces of the adjacent units, the vertex of the right angle of one triangular face coincides with the center point of the longest edge of the other triangular face.

The rigid-folding mechanisms of the proposed structure are evaluated using the panel-pin model proposed in our previous study [8]. As demonstrated in Section 2, a single unit has two-degrees-of-freedom first-order infinitesimal rigid-folding mechanisms which are the potential finite mechanisms. On the other hand, as demonstrated in Section 3, a structure with three units in both directions of the grid has a single-degree-of-freedom first-order infinitesimal rigid-folding mechanism corresponding to the *primary path* shown in Fig. 2 which connects two flat-folded states. On the primary path, there is a singular state where all folding angles are equal and the number of degrees of freedom of the rigid-folding mechanism increases by one. The path obtained from the additional degree of freedom is referred to as the *bifurcation path* [9] in this study. This additional mechanism is, however, shown to be only the first-order infinitesimal mechanism that does not lead the finite deformation. The assignment of the panel thickness is also considered in Section 4. The panel thickness can be easily assigned by just offsetting the faces to the outside direction of the units while the rigid-folding mechanism is preserved. By utilizing the finite mechanism described above, the structure can be compactly stored in a flat state and stably deployed. Furthermore, although only infinitesimal mechanisms are investigated and the effects of gravity and materials are not accounted for in this paper, the out-of-plane mechanism in the singular state is expected to be used to realize the curved surface structure as illustrated in Fig. 3 by allowing the small elastic deformation of panels when ultra-lightweight and stiff materials are available.

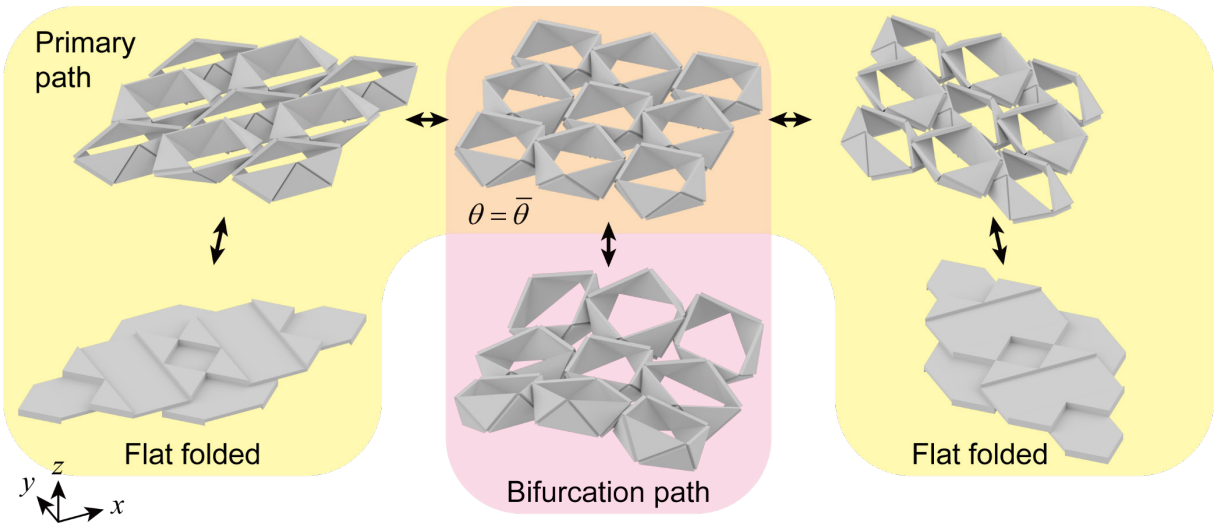


Figure 2. Overview of folding process of the proposed 3×3 unit structure. The structure has a single-degree-of-freedom finite rigid-folding path referred to as the primary path and a first-order infinitesimal mechanism in the singular state $\theta = \bar{\theta}$ referred to as the bifurcation path.

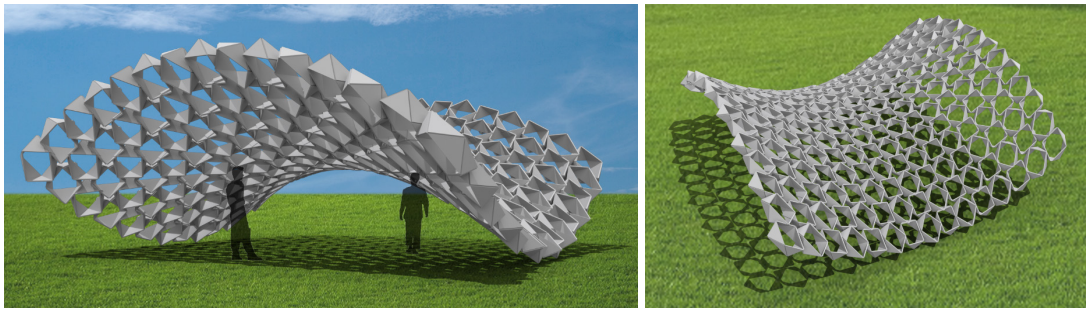

Figure 3. Possible future application of the proposed structure to the curved roof structure expected to be realized when ultra-lightweight and stiff materials are available.

## 2. Geometry and kinematics of single unit

### 2.1. Analytical solution to primary path

In this section, the rigid-folding deformation of a single unit on the primary path is analytically described, and the infinitesimal mechanism of the single unit is investigated using the panel-pin model [8]. In the following, the length of the base and the height of each right-angled isosceles triangle are $2a$ and $a$, respectively, as shown in Fig. 1. The thickness of each panel is irrelevant to the folding mechanism of the single unit investigated in this section.

When vertices A, B, C, and D of a single unit form a square as shown in Fig. 1(a), we place the origin of the coordinate system for the unit at the center of square ABCD and set the *x*- and *y*-axes in the directions of the vector pointing vertices D from C and the vector pointing vertices A from D, respectively. Let $\theta$ and $\varphi$ denote the angle between face ADE and the *xy*-plane and between face ABF and the *xy*-plane, respectively. Under the assumption that vertices A–D do not move, these angles $\theta$ and $\varphi$ satisfy the following equation so that the length of edge EF does not change:

$$a^2\left[\left(1+\cos\theta\right)^2+\left(1+\cos\varphi\right)^2+\left(\sin\theta-\sin\varphi\right)^2\right]=4a^2 \Leftrightarrow \cos\theta+\cos\varphi-\sin\theta\sin\varphi=0 \tag{1}$$

Equation (1) can be solved for $\varphi$ as follows:

$$\varphi=\begin{cases}\pi & \left(\theta=0\right)\\ 2\tan^{-1}\left(\left(\sqrt{2}-1\right)\cot\dfrac{\theta}{2}\right) & \left(0<\theta<\pi\right)\\ 0 & \left(\theta=\pi\right)\end{cases} \tag{2}$$

Therefore, $\varphi$ is determined uniquely by $\theta$. The similar relationships hold for the pairs of faces ABF and BCG, faces BCG and CDH, and faces CDH and ADE. Consequently, if vertices A–D do not move, the angles between face BCG and the *xy*-plane and between face CDH and the *xy*-plane are also $\theta$ and $\varphi$, respectively, from the compatibility conditions of the angles of the faces for the entire unit. This implies that the unit has the single-degree-of-freedom finite mechanism expressed as Eq. (2) when vertices A–D form a square and do not move. This finite mechanism is preserved when the multiple units are connected as described in Section 1 and Fig. 2, and we refer to the rigid-folding path along this finite mechanism as the primary path. Especially when $\theta=\varphi$ and vertices E, F, G, and H also form the square parallel to that formed by vertices A–D, let $\theta=\bar{\theta}$ that is referred to as the singular state. From Eq. (2), $\bar{\theta}$ is calculated as $\bar{\theta}=2\tan^{-1}\sqrt{\sqrt{2}-1}\simeq 1.144$ rad. $\rightarrow 65.53$ deg.

### 2.2. Outline of infinitesimal mechanism analysis using panel-pin model

The infinitesimal mechanism of the single unit is analyzed using the panel-pin model [8]. This model consists of rigid panels pin-connected to each other at their vertices. The folding deformation of the rigid

origami is represented by the translational and rotational displacements of the centers of gravity of panels. These panel displacements are treated as variables in the analysis under the compatibility conditions so that the translational displacements of the connected panel vertices are the same in the deformation process of the model. The detailed formulation of the compatibility condition for each pair of connected vertices can be found in Ref. [8].

Let $N_\mathrm{p}$ and $N_\mathrm{c}$ denote the number of panels and crease lines, respectively. The translational and rotational displacements of all the panels in the panel-pin model are assembled into the *generalized displacement vector* $\mathbf{X} \in \mathbb{R}^{6N_\mathrm{p}}$. Then, the compatibility condition for the entire model is represented using the incompatibility vector $\mathbf{C}(\mathbf{X}) \in \mathbb{R}^{6N_\mathrm{c}}$, which is the assemblage of the incompatibility of the displacements of the connected vertices, as follows:

$$\mathbf{C}(\mathbf{X}) = \mathbf{0} \tag{3}$$

Note that the support condition of the model is not considered in this paper, and the rigid-body motion of the model is allowed. We assume $\mathbf{X} = \mathbf{0}$ in each folded state on the primary path determined by specifying the value of $\theta$, and the first-order infinitesimal mechanism of the panel-pin model is evaluated at $\mathbf{X} = \mathbf{0}$. When the $i$-th component of $\mathbf{C}(\mathbf{X})$ and the $j$-th component of $\mathbf{X}$ are denote by $C_i(\mathbf{X})$ $(i = 1,\ldots,6N_\mathrm{c})$, and $X_j$ $(j = 1,\ldots,6N_\mathrm{p})$, respectively, the *compatibility matrix* $\mathbf{\Gamma} \in \mathbb{R}^{6N_\mathrm{c} \times 6N_\mathrm{p}}$ is defined as the matrix whose $(i, j)$ component is $\partial C_i(\mathbf{0}) / \partial X_j$ $(i = 1,\ldots,6N_\mathrm{c};\ j = 1,\ldots,6N_\mathrm{p})$. From the first-order differentiation of Eq. (3), the *first-order infinitesimal mechanism* of the panel-pin model at $\mathbf{X} = \mathbf{0}$ is represented by the vector $\mathbf{X}' \in \mathbb{R}^{6N_\mathrm{p}}$ satisfying

$$\mathbf{\Gamma X}' = \mathbf{0} \tag{4}$$

The solution space of Eq, (4) is $\ker \mathbf{\Gamma}$ whose dimension is $N_\mathrm{f} = 6N_\mathrm{p} - \operatorname{rank} \mathbf{\Gamma}$. Here, $N_\mathrm{f}$ is referred to as the *number of kinematic indeterminacies*, and the bases of $\ker \mathbf{\Gamma}$ is referred to as the *infinitesimal mechanism modes,* which include the six degrees of freedom of the rigid-body motions because the support condition is not assigned. Consequently, the degrees of freedom of the rigid-folding mechanisms are $N_\mathrm{f} - 6$ for the panel-pin model.

We also investigate the existence condition of the second-order infinitesimal mechanism in each folded state. The second-order infinitesimal mechanism is represented by the pair $(\mathbf{X}', \mathbf{X}'') \in (\mathbb{R}^{6N_\mathrm{p}}, \mathbb{R}^{6N_\mathrm{p}})$ satisfying the following equations obtained by twice differentiating Eq. (3) [8, 9]:

$$\begin{cases} \mathbf{\Gamma X}' = \mathbf{0} \\ \mathbf{\Gamma X}'' + \mathbf{H X}' = \mathbf{0} \end{cases} \tag{5}$$

where $\mathbf{H} \in \mathbb{R}^{6N_\mathrm{c} \times 6N_\mathrm{p}}$ is the matrix whose $(i, j)$ component is $\sum_{k=1}^{6N_\mathrm{p}} \left( \partial^2 C_i(\mathbf{0}) / \partial X_j \partial X_k \right) X'_k$ $(i = 1,\ldots,6N_\mathrm{c};\ j = 1,\ldots,6N_\mathrm{p})$, and $X'_k$ is the $k$-th component of $\mathbf{X}'$ $(k = 1,\ldots,6N_\mathrm{p})$. The condition for the existence of $\mathbf{X}''$ satisfying Eq. (5) with non-zero $\mathbf{X}'$ is that $\mathbf{H X}'$ is orthogonal to all the bases of $\ker \mathbf{\Gamma}^\mathrm{T}$ whose dimension is $N_\mathrm{s} = 6N_\mathrm{c} - \operatorname{rank} \mathbf{\Gamma}$. Here, $N_\mathrm{s}$ is referred to as the *number of statical indeterminacies*, and the bases of $\ker \mathbf{\Gamma}^\mathrm{T}$ is referred to as the *self-equilibrium force modes*. Since $\mathbf{H X}'$ is the quadratic form with respect to $\mathbf{X}'$, the existence condition for the second-order infinitesimal mechanism is a system of $N_\mathrm{s}$ quadratic equations for $\mathbf{X}'$ satisfying Eq. (4) [8, 9].

### 2.3. Results of infinitesimal mechanism analysis

The singular values of the compatibility matrix $\mathbf{\Gamma}$ are investigated in each folded state on the primary path by varying the value of $\theta$ in the range of $0.001\pi \le \theta \le 0.999\pi$. In the case of the single unit, eight singular values are less than $10^{-14}$ and the remaining singular values are greater than $10^{-4}$ regardless of the value of $\theta$. Since the size of $\mathbf{\Gamma}$ is $48 \times 48$, the rank of $\mathbf{\Gamma}$ is 40 [10], and the degrees of freedom of

the rigid-folding mechanisms are two excluding the rigid-body motion.

In addition, there are eight quadratic equations for the existence of the second-order infinitesimal mechanism obtained from the eight self-equilibrium force modes. All the rigid-folding modes in each folded state on the primary path satisfy these quadratic equations for all $\theta$, and we can conclude that the single unit on the primary path has two-degrees-of-freedom rigid-folding mechanisms that are the potential finite mechanisms.

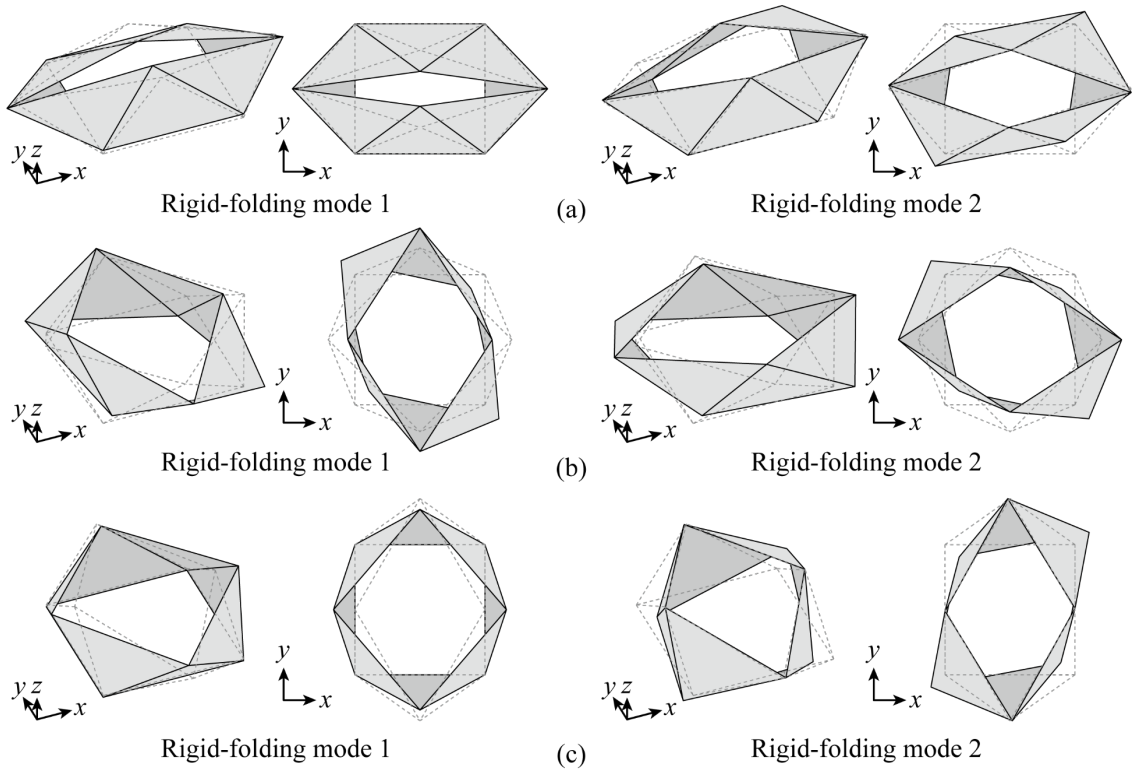


Figure 4. First-order infinitesimal mechanism modes of a single unit at (a) $\theta \simeq 30.12\,\mathrm{deg.}$, (b) $\theta = \overline{\theta} \simeq 65.53\,\mathrm{deg.}$, and (c) $\theta \simeq 90.00\,\mathrm{deg.}$

Figure 4 illustrates the first-order infinitesimal mechanism modes of the single unit excluding the rigid-body motions at $\theta \simeq 30.12\,\mathrm{deg.}$, $\theta = \overline{\theta} \simeq 65.53\,\mathrm{deg.}$, and $\theta \simeq 90.00\,\mathrm{deg.}$ When $\theta \simeq 30.12\,\mathrm{deg.}$ and $\theta \simeq 90.00\,\mathrm{deg.}$, one mode corresponds to the primary path, and the other mode corresponds to the twisting motion of the unit. On the other hand, when $\theta = \overline{\theta}$, both of two infinitesimal modes are the mixture of the deformation modes in two possible primary paths where the bottom four vertices or the top four vertices are fixed.

## 3. Infinitesimal mechanism of 3×3 unit structure without panel thickness

The infinitesimal mechanism of the structure with three units in both directions of the grid, referred to as the 3×3 unit structure, is evaluated using the panel-pin model. Each folded state on the primary path is investigated in the range of $0.001\pi \le \theta \le 0.999\pi$, and we show that the number of kinematic indeterminacies increases in the singular state $\theta = \overline{\theta}$. In this section, thickness of the panel is neglected.

Because the glued panels of the adjacent units have the same translational and rotational displacement, the panel displacements in each pair of glued panels are expressed using the common variables in the panel-pin model. Thus, the number of components in the generalized displacement vector **X** is calculated as $6\times\left(8\times3\times3-2\times3\times2\right)=6\times60=360$, and the number of components in the

incompatibility vector $\mathbf{C}(\mathbf{X})$ is $6\times8\times3\times3=6\times72=432$. When $\theta\neq\overline{\theta}\simeq65.53\,\mathrm{deg.}$, there are seven singular values of compatibility matrix $\boldsymbol{\Gamma}$ which are less than $10^{-14}$, and the remaining singular values are greater than $10^{-9}$. Therefore, the rank of $\boldsymbol{\Gamma}$ can be regarded as 353, and the numbers of kinematic and statical indeterminacies are 7 and 79, respectively, when $\theta\neq\overline{\theta}$. On the other hand, when $\theta=\overline{\theta}$, eight singular values are less than $10^{-14}$, and the remaining singular values are greater than $10^{-2}$. This implies that the numbers of kinematic and statical indeterminacies increase by 1, respectively, from the other folded state. The first-order infinitesimal mechanisms excluding the rigid-body motions are shown in Fig. 5 for $\theta\simeq30.12\,\mathrm{deg.}$, $\theta=\overline{\theta}\simeq65.53\,\mathrm{deg.}$, and $\theta\simeq90.00\,\mathrm{deg.}$

The existence condition of the second-order infinitesimal mechanism is also investigated in each folded state. When $\theta\neq\overline{\theta}$, the single-degree-of-freedom first-order infinitesimal mechanism excluding the rigid-body motions satisfies all the quadratic equations, and we can conclude that this first-order infinitesimal mechanism can be extended to the second-order infinitesimal mechanism and the finite mechanism as well. This is also supported by the infinitesimal mechanism modes at $\theta\simeq30.12\,\mathrm{deg.}$ and $\theta\simeq90.00\,\mathrm{deg.}$ shown in Fig. 5 corresponding to the deformation in the primary path. On the other hand, when $\theta=\overline{\theta}$, one of the two infinitesimal mechanism modes excluding the rigid-body motions satisfies the quadratic equations for the existence of the second-order infinitesimal mechanism while the other mode does not. The mode satisfying the existence condition of the second-order infinitesimal mechanism is the rigid-folding mode 2 in Fig. 5(b) corresponding to the deformation in the primary path. The other mode is the rigid-folding mode 1 in Fig. 5(b) and corresponds to the out-of-plane deformation of the 3×3 unit structure. This mode forms the bifurcation path in Fig. 2, and the deformation in this direction cannot occur in the range of the large displacement without panel deformation.

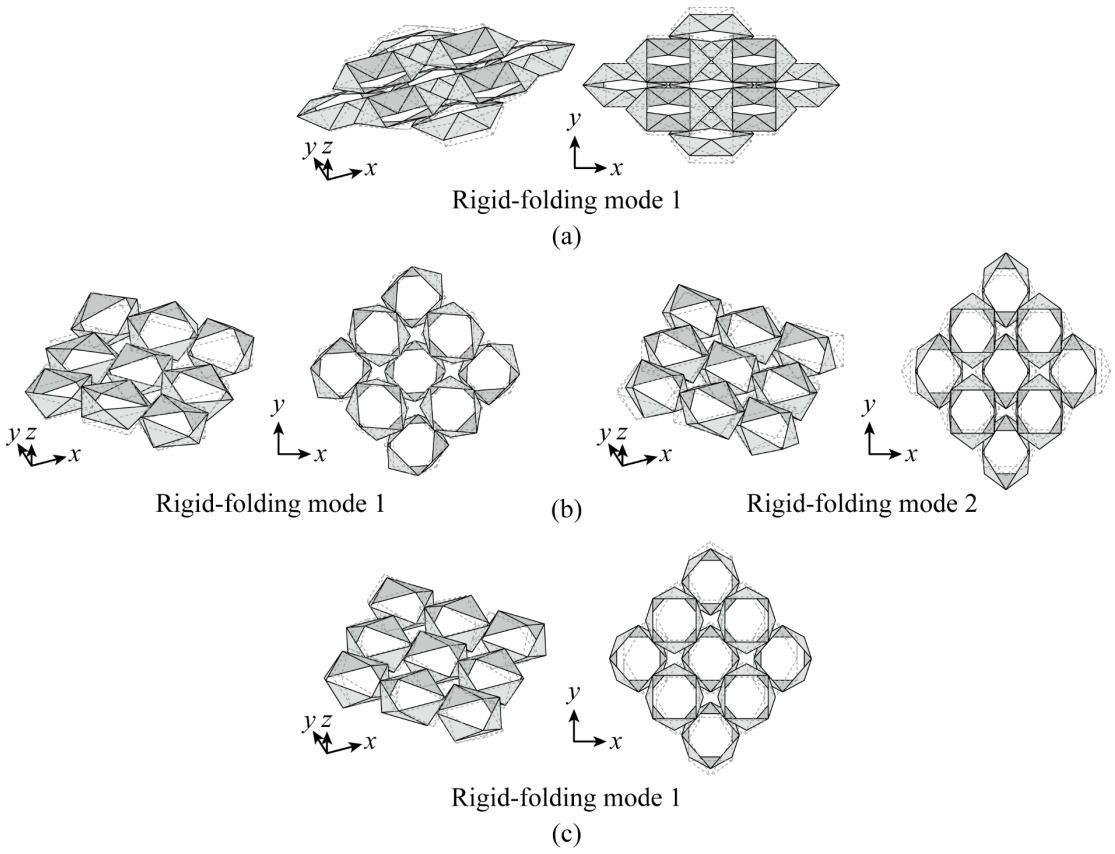


Figure 5. First-order infinitesimal mechanism modes of a 3×3 unit structure at (a) $\theta\simeq30.12\,\mathrm{deg.}$, (b) $\theta=\overline{\theta}\simeq65.53\,\mathrm{deg.}$, and (c) $\theta\simeq90.00\,\mathrm{deg.}$

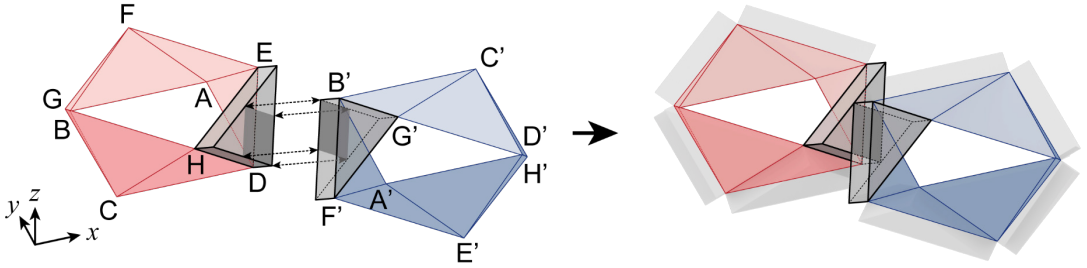


Figure 6. Assignment of panel thickness.

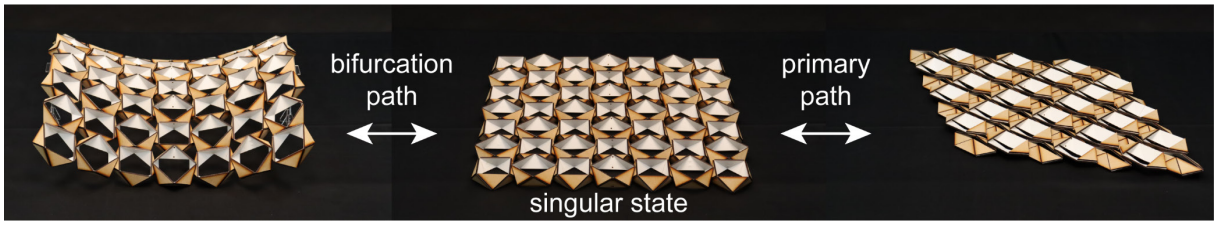


Figure 7. Model with thick panels. Materials of panels and hinges are medium density fiberboard (MDF) and paper, respectively.

## 4. Assignment of panel thickness

This section shows the assignment of the panel thickness and the connectivity of the units with the panel thickness. As shown in Figs. 2 and 6, the panel thickness is uniformly assigned in the outward normal direction of each face of the unit. When the thickness is assigned in this way, the rigid-folding mechanism of a single unit is the same as when the thickness is not considered, except for the contact of the panels in the flat state.

The adjacent units are connected as in the case where the panel thickness is neglected. As shown in Fig. 6, the adjacent units consisting of vertices A–G and vertices A'–G', respectively, which are in the inverted orientation to each other, are connected between the panels obtained by offsetting faces DEH and B'F'G'. These panels are referred to as the panels DEH and B'F'G', respectively, for brevity. The adjacent units are connected so that the following conditions are satisfied:

- The outer faces of panels DEH and B'F'G' are glued together.
- The vertex of the panel obtained by offsetting vertex D meets the center point of the edge of the panel obtained by offsetting edge F'G'.
- The vertex of the panel obtained by offsetting vertex B' meets the center point of the edge of the panel obtained by offsetting edge EH.

When the units are connected in this manner, the layout of the crease lines within each unit is the same as in the case without panel thickness, and the relative position and orientation of the crease lines between the units are determined by simply translating the units from the arrangement without panel thickness. Therefore, although the initial relative positions between the glued panels are different from the case where thickness is ignored, the translational and rotational displacements of these panels remain identical. This leads to the same formulation of the panel-pin model between the cases with and without the thickness of the panels, and the infinitesimal mechanisms of the model are not influenced by the assignment of the panel thickness.

We made a physical model by using the method proposed here as shown in Fig. 7. There are 7×7 units, and each unit consists of the 3 mm thickness panels with the bases of length $2a = 60$ mm. The panels are made of medium density fiberboard (MDF) connected by paper hinges. As demonstrated in Section 3, this model has the rigid-folding modes corresponding to the primary path between the two flat folded state and the bifurcation path showing the out-of-plane deformation that approximates a surface with

negative Gaussian curvature. Although the mechanism corresponding to the bifurcation path is only the first-order infinitesimal mechanism, relatively large deformation occurs in this direction with small elastic deformation at the hinges compared to the other out-of-plane directions.

## 5. Conclusions

In this study, we present the origami-based structure that is rigid- and flat-foldable. A finite rigid-folding path of the single unit is analytically derived, and the infinitesimal mechanisms of the single unit and the 3×3 unit structure are investigated using the panel-pin model. It is shown from the infinitesimal mechanism analysis that the single unit has two first-order infinitesimal mechanism modes that are the potential finite mechanisms, and the 3×3 unit structure has one first-order infinitesimal mechanism mode corresponding to the finite folding path connecting two flat-folded states. At the singular state, the 3×3 unit structure also has one first-order infinitesimal mechanism that does not satisfy the existence condition of the second-order infinitesimal mechanism. This mode shows the out-of-plane deformation approximating a surface with negative Gaussian curvature. These properties are also confirmed in the physical model with 7×7 units.

## Acknowledgements

This work is supported by JSPS KAKENHI Grant Number JP23K19160 and JST CREST Grant Number JPMJCR1911.

## References

[1] H. Yasuda, T. Yein, T. Tachi, K. Miura, and M. Taya, “Folding behaviour of Tachi-Miura polyhedron bellows,” *Proceedings of the Royal Society A: Mathematical, Physical, and Engineering Sciences*, vol. 469, no. 2159, paper no. 20130351, 2013.

[2] E. T. Filipov, G. H. Paulino and T. Tachi, “Origami tubes with reconfigurable polygonal cross-sections,” *Proceedings of the Royal Society A: Mathematical, Physical, and Engineering Sciences*, vol. 472, no. 2185, paper no. 20150607, 2016.

[3] J. E. Suh, T. H. Kim, and J. H. Han, “New approach to folding a thin-walled Yoshimura patterned cylinder,” *Journal of Spacecraft and Rockets*, vol. 58, no. 2, pp. 516–530, 2021.

[4] K. Saito, S. Pellegrino, and T. Nojima, “Manufacture of arbitrary cross-section composite honeycomb cores based on origami techniques,” *Journal of Mechanical Design*, vol. 136, no. 5, paper no. 051011, 2014.

[5] J. M. Gattas and Z. You, “Geometric assembly of rigid-foldable morphing sandwich structures,” *Engineering Structures*, vol. 94, pp. 149–159, 2015.

[6] R. Ma, M. Li, Y. Xu, M. Meloni, J. Feng, and J. Cai, “Geometry design and in-plane compression performance of novel origami honeycomb material,” *Thin-Walled Structures*, vol. 181, paper no. 110111, 2022.

[7] R. Maleczek and C. Genevaux, “Design constraints for linear folded strips,” *International Journal of Space Structures*, vol. 30, no. 2, pp. 179–190, 2015.

[8] K. Hayakawa and M. Ohsaki, “Panel-pin model for kinematic and equilibrium analysis of rigid origami,” *Journal of the International Association for Shell and Spatial Structures,* vol. 64, no. 4, pp. 278–288, 2023.

[9] P. Kumar and S. Pellegrino, “Computation of kinematic paths and bifurcation points,” International Journal of Solids and Structures, vol. 37, no. 46, pp. 7003–7072, 2000.

[10] C. D. Meyer, *Matrix Analysis and Applied Linear Algebra*, SIAM, 2000.